



This is a repository copy of *A pressure swing approach to selective CO<sub>2</sub> sequestration using functionalised hypercrosslinked polymers.*

White Rose Research Online URL for this paper:  
<http://eprints.whiterose.ac.uk/151506/>

Version: Submitted Version

---

**Article:**

James, A.M., Reynolds, J., Reed, D.G. et al. (2 more authors) (Accepted: 2019) A pressure swing approach to selective CO<sub>2</sub> sequestration using functionalised hypercrosslinked polymers. ChemRxiv. (Submitted)

10.26434/chemrxiv.9896873.v1

---

**Reuse**

This article is distributed under the terms of the Creative Commons Attribution-NonCommercial-NoDerivs (CC BY-NC-ND) licence. This licence only allows you to download this work and share it with others as long as you credit the authors, but you can't change the article in any way or use it commercially. More information and the full terms of the licence here: <https://creativecommons.org/licenses/>

**Takedown**

If you consider content in White Rose Research Online to be in breach of UK law, please notify us by emailing [eprints@whiterose.ac.uk](mailto:eprints@whiterose.ac.uk) including the URL of the record and the reason for the withdrawal request.



[eprints@whiterose.ac.uk](mailto:eprints@whiterose.ac.uk)  
<https://eprints.whiterose.ac.uk/>

# A pressure swing approach to selective CO<sub>2</sub> sequestration using Functionalised Hypercrosslinked Polymers

Alex M. James,<sup>a</sup> Jake Reynolds,<sup>a</sup> Dan G. Reed,<sup>b</sup> Peter Styring<sup>b</sup> and Robert Dawson<sup>\*a</sup>

Functionalised hypercrosslinked polymers (HCPs) with surface areas between 213 – 1124 m<sup>2</sup>/g based on a range of monomers containing different chemical moieties are evaluated for CO<sub>2</sub> capture using a pressure swing adsorption (PSA) methodology under humid conditions and elevated temperatures. The networks demonstrated rapid CO<sub>2</sub> uptake reaching maximum uptakes in under 60 seconds. The most promising networks demonstrating the best selectivity and highest uptakes were applied to a pressure swing setup using simulated flue gas streams. The carbazole, triphenylmethanol and triphenylamine networks were found to be capable of converting a dilute CO<sub>2</sub> stream (> 20 %) into a concentrated stream (> 85 %) after only two pressure swing cycles from 20 bar (adsorption) to 1 bar (desorption). This work demonstrates the ease by which readily synthesised functional porous materials can be successfully applied to a pressure swing methodology and used to separate CO<sub>2</sub> from N<sub>2</sub> from industrially applicable simulated gas streams under more realistic conditions.

## Broader Context

The capture of carbon dioxide emissions from power generation and industry are a major challenge in the effort to prevent irreversible climate change. Porous materials are one potential solution due to their high surface areas and tunability of the interactions between the adsorbent surface and CO<sub>2</sub> *via* chemical functionalisation. In comparison with traditional chemical binding of CO<sub>2</sub> (chemisorption), the relatively weak physical interaction between the porous materials' surface and CO<sub>2</sub> (physisorption) allows the adsorbent to be easily recycled. Most previous studies using porous materials have used the difference in temperature between the adsorption and desorption processes for the regeneration of the adsorbent (temperature swing), however this process comes with a significant energy penalty. In this study we investigate the use of a lower energy pressure swing process. Here, the adsorbent is loaded with a simulated mixture of flue gas at high pressure. Over a series of decompression steps, the released gas mixture can be enriched in CO<sub>2</sub> due to its preferential binding to the adsorbent.

## Introduction

The 2015 Paris Agreement aims to limit the average global temperature increase to 2°C. One of the key causes of climate change is anthropogenic carbon dioxide, and recently the UK government has committed to a net zero emissions target by 2050. In the long term the most effective method to lower carbon dioxide (CO<sub>2</sub>) emissions is to switch to renewable energy sources. However, the transition to renewable energy such as solar and wind is likely to take decades hence the continued reliance on non-sustainable energy sources.<sup>1,2</sup> In order to meet the short to medium term emissions targets, the capture, storage and utilisation of CO<sub>2</sub> from large anthropogenic point sources such as fossil fuel power plants and the steel industry, is key to mitigating the ever increasing levels of CO<sub>2</sub> in the atmosphere thereby preventing irreversible climate change.<sup>3</sup>

One of the key challenges facing materials for carbon capture from anthropogenic point sources is the low

concentration of CO<sub>2</sub> in flue gas streams is often around or lower than 20%. The remaining volume is comprised largely of N<sub>2</sub> with smaller amounts of water vapour, oxygen, SO<sub>2</sub> and NO<sub>x</sub> (amongst others).<sup>4</sup> In order to capture CO<sub>2</sub> efficiently, any capture process therefore needs to show high selectivity towards CO<sub>2</sub>.

The current state-of-the-art industrial method of capturing CO<sub>2</sub>, dubbed amine scrubbing, has remained unchanged for decades and involves the use of aqueous solutions of amines such as monoethanolamine (MEA) as shown in figure 1a.<sup>5</sup> This process relies on chemisorption, by which the MEA selectively reacts with CO<sub>2</sub> to form a carbamate salt.

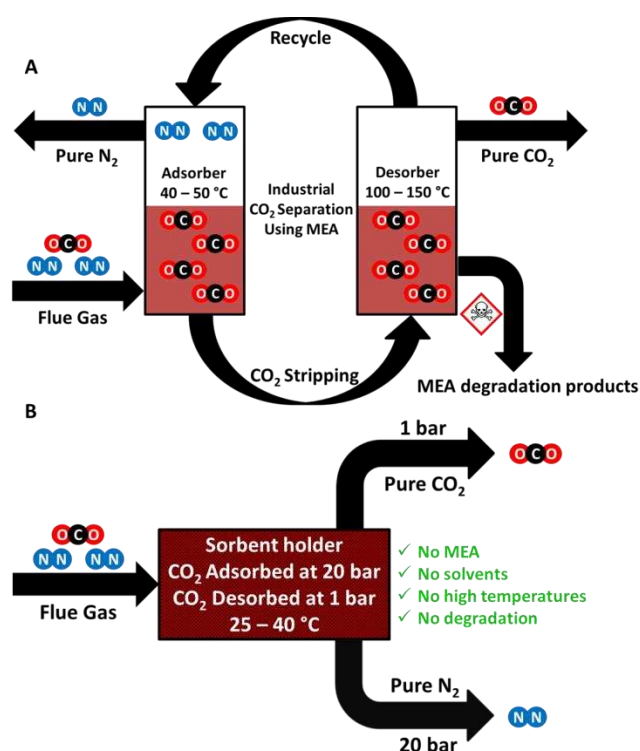


**Figure 1.** (a) Simplified industrial CO<sub>2</sub> capture process using MEA as a liquid sorbent to separate out CO<sub>2</sub> from industrial flue gas. (b) The ideal pressure swing approach which could be utilised to separate out CO<sub>2</sub> from flue gas mixtures.

Over the past few years there has been a move away from the amine scrubbing process due to significant and numerous drawbacks. These include the chemisorption process requiring very high temperatures (ca. 130 °C) to liberate the CO<sub>2</sub> and regenerate the free amine. Attaining these high temperatures is a challenge for industry and comes at a high price both fiscally and environmentally. Nonsensically in order to power this process one has to produce CO<sub>2</sub> to capture CO<sub>2</sub>.<sup>6</sup> Other issues include the corrosive nature of the amine solution along with the sensitivity of such solvents to other gaseous impurities present in the flue gas such as SO<sub>x</sub> and NO<sub>x</sub>.<sup>7-9</sup> This results in continuous degradation as well as evaporation meaning the amine solution needs to be changed on a regular basis thereby raising the operating cost of the process.<sup>10</sup> Due to the difference in the temperature at which the reaction of amines and CO<sub>2</sub> react compared to the temperature required to regenerate the amine, this process is known as a temperature swing approach. Due to the high energy penalty required by the regeneration temperature, this method is not ideal for the capture of CO<sub>2</sub>. In contrast, a physisorption process, whereby the interaction between adsorbent and adsorbate is weaker yet still significant enough for the binding of CO<sub>2</sub> to the substrate surface, requires much less energy to regenerate the free material and liberate the pure gas.<sup>3,8</sup>

Most reports of new materials for carbon capture use a temperature swing approach. There is much less literature relating to adsorbents using the alternative pressure swing approach. Pressure swing adsorption (PSA) technology is a growing body of research which is compatible with solid sorbents and has the potential to optimise and replace the current temperature swing technologies applied in industry.<sup>11,12</sup> In a pressure swing approach CO<sub>2</sub> is adsorbed at high pressures by a solid sorbent before being desorbed at low pressures (figure 1b), or under slight vacuum (VPSA). Different sorbents require different pressure profiles but are typically around 10-30 bar in the adsorption cycle. In comparison to temperature swing, PSA is an inherently low energy technique for which high temperatures are not required during adsorption or desorption. PSA is also a much faster technique compared to temperature swing as there is no thermal lag meaning that the adsorb/desorb cycle can be performed rapidly. There is much scope for variation with PSA such as optimisation of the sorbent, the working pressures and temperatures of the process, all of which can be varied to yield the most efficient and effective system.

In order for a material to be considered a viable choice as a solid sorbent for pressure swing adsorption, certain criteria have to be met. These include; the material being stable and selective towards CO<sub>2</sub> at both low and high pressures. The material must demonstrate good recyclability over many pressure cycles. Furthermore, it is desirable to be both cheap and relatively simple to make with good yields due to the scale of the process and to keep the cost low.

Over the last two decades, as interest in carbon dioxide capture/utilisation, CCS/CCU, has accelerated numerous sorbents demonstrating CO<sub>2</sub> capturing capabilities have been reported mainly using the temperature swing approach.<sup>3,7,8,13</sup>

These include zeolites,<sup>14</sup> hybrid materials such as metal organic frameworks (MOFs),<sup>15</sup> activated carbons, ionic liquids,<sup>16,17</sup> and microporous organic polymers (MOPs).<sup>18-24</sup>

MOPs are a family of porous materials comprised solely of the lighter elements of the periodic table. There are a large number of different sub-classes of MOP such as; conjugated microporous polymers (CMPs)<sup>25-27</sup>, covalent organic frameworks (COFs)<sup>28-31</sup>, covalent triazine frameworks (CTFs)<sup>32,33</sup>, polymers of intrinsic microporosity (PIMs)<sup>34-37</sup> which have been applied to various applications ranging from chemosensing,<sup>32,38-40</sup> catalysis<sup>41-44</sup> and waste water treatment.<sup>45-48</sup> CO<sub>2</sub> uptakes of MOPs are typically measured at conditions of around 1 bar and at temperatures ranging from 273-298 K. Some of the best performing MOPs include functionalised networks containing amine groups with uptakes of around 15-20 wt. % at 1 bar and 273 K.<sup>49,50</sup> At higher pressures materials such as PAF-1 and PPN-4 have a reported uptake of 130 wt. % (40 bar, 298 K)<sup>51</sup> and 212 wt. % (50 bar, 295 K)<sup>52</sup> respectively. However, one class of MOP stands out for the application of carbon dioxide capture due to their low skeletal density, chemically and thermally stability and synthesis using cheap, readily available starting materials on a large scale – hypercrosslinked polymers (HCPs).<sup>20-22,53</sup> At high pressures there are however relatively few studies. HCPs based on 4,4'-bis(chloromethyl)-1,1'-biphenyl (BCMBP) were shown to have uptakes of up to 58.7 wt. % at 30 bar.<sup>21</sup> While this falls short of the PAF/PPN materials, HCP synthesis is considerably less complex and cheaper.

Hypercrosslinked polymers are rigid porous networks with typical surface areas in the range of 500-2000 m<sup>2</sup>/g.<sup>54-56</sup> Their synthesis is often based on Friedel-Crafts chemistry using a Lewis-acid catalysts such as iron (iii) chloride to yield a highly crosslinked and permanently microporous insoluble solid product. HCP synthesis requires the use of crosslinking groups, such as methyl chlorides often dubbed “internal crosslinkers”,<sup>57,58</sup> or external crosslinkers such as formaldehyde dimethyl acetal (FDA).<sup>59</sup> This external “knitting method” allows potentially any rigid aromatic monomer to be hypercrosslinked.

Crucially the “knitting method” provides a route to the incorporation of a range of chemical functionalities into the networks by polymerisation of pre-functionalised monomers. This has led to the investigation of HCPs for a variety of different applications.<sup>20,60-62</sup> For CO<sub>2</sub> capture it is well known that different chemical moieties can impart increased selectivity towards CO<sub>2</sub> over other gases due to more favourable interactions with the chemical moiety and the dipole of the CO<sub>2</sub>.<sup>24,63-65</sup> These interactions are crucial to maximising their selectivity towards CO<sub>2</sub>.

In this work we report the synthesis, characterisation and implementation of functional HCP networks for use as solid sorbents using a PSA approach. The CO<sub>2</sub> uptake capacity and uptake kinetics are measured at high pressure followed by measurements using simulated flue gas compositions. The CO<sub>2</sub>:N<sub>2</sub> selectivity of the materials is calculated and the recyclability potential of the HCPs is evaluated. Further to this, in order to keep the study industrially applicable all samples were exposed to simulated gas streams and the materials themselves were exposed to the humid laboratory conditions and not used straight out of the oven.

## Experimental

### Materials

Anhydrous 1,2-dichloroethane (DCE, > 99%), iron (III) chloride (FeCl<sub>3</sub>, 97%) and formaldehyde dimethyl acetal (FDA, >99%), BINOL (>99%), dibenzyl ether (>99%) and poly(styrene) (M<sub>n</sub>=280 000 g/mol) were all purchased from Sigma-Aldrich. Triphenylmethanol (Lancaster synthesis, >99%), carbazole (Alfa Aesar, 95%) and triphenylamine (Fluorochem >99%) were used as received. All chemicals were used as received unless stated otherwise.

### Synthesis of HCPs

Hypercrosslinked porous polymers were synthesised via the “knitting route” using functional aromatic monomers. All reactions were performed under a nitrogen atmosphere (see Table S1 for quantities). Using triphenylmethanol as an example; triphenylmethanol (3.00 g, 11.54 mmol, 1 eq.) was added to a 2-necked round bottom flask which was degassed by three freeze-pump-thaw cycles. To this vessel DCE (60 mL) and FDA (7.65 mL, 86.57 mmol, 7.5 eq.) were added along with a slurry of FeCl<sub>3</sub> (14.02 g, 86.57 mmol, 7.5 eq.) in DCE. The reaction was heated to 80 °C and left for 16 h to afford a solid black product. The crude black product was washed and filtered with methanol before being solvent extracted with methanol using Soxhlet apparatus overnight. The black solid was washed and filtered with chloroform and methanol before being left to dry overnight under vacuum at 60 °C.

### Characterisation

Fourier transform infrared (FTIR) spectroscopy was performed using a Perkin-Elmer Spectrum 100 fitted with an attenuated total reflectance tip (ATR). Solid-State NMR samples were packed into 4 mm zirconia rotors and transferred to a Bruker Avance III HD spectrometer. 1D <sup>1</sup>H-<sup>13</sup>C cross-polarisation magic angle spinning (CP/MAS) NMR experiments were measured at 125.76 MHz (500.13 MHz <sup>1</sup>H) at a MAS rate of 10.0 kHz. The <sup>1</sup>H π/2 pulse was 3.4 μs, and two-pulse phase modulation (TPPM) decoupling was used during the acquisition. The Hartmann-Hahn condition was set using hexamethylbenzene. The spectra were measured using a contact time of 2.0 ms. The relaxation delay D<sub>1</sub> for each sample was individually determined from the proton T<sub>1</sub> measurement (D<sub>1</sub> = 5 × T<sub>1</sub>). Samples were collected until sufficient signal to noise was observed, typically greater than 256 scans. The values of the chemical shifts are referred to that of TMS. Gas sorption measurements were performed using

a Micromeritics ASAP 2020 Plus analyser employing high purity gases. Approximately 100 mg of sample was degassed at 120 °C for 16 h under dynamic vacuum immediately prior to analysis. BET surface areas were calculated using nitrogen gas at 77 K over a pressure range of 0.01-0.15 P/P<sub>0</sub>.

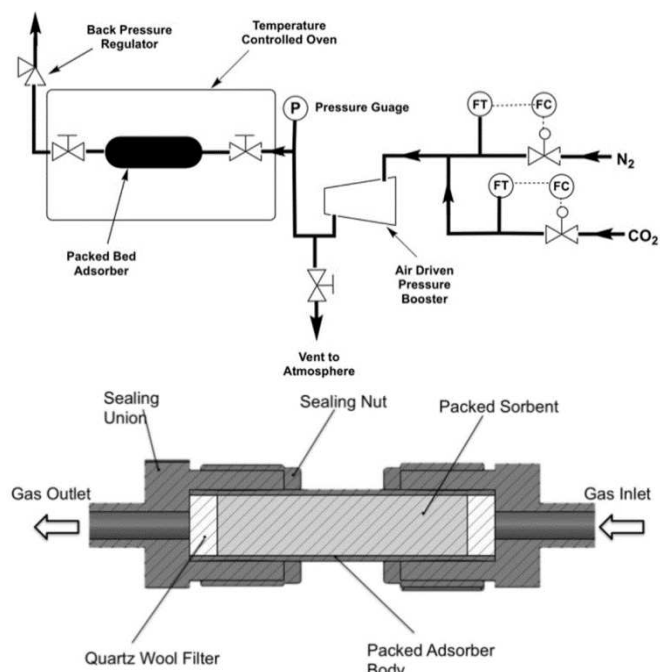


**Figure 2.** (Above) Simplified flow diagram of the experimental apparatus setup used during the high pressure testing. (Below) Cross-sectional view of the packed-bed adsorber used for CO<sub>2</sub> separation at high pressures. Figures reproduced with permission from ref. <sup>66</sup>. Copyright 2017, Reed, Dowson and Styring.

High pressure adsorption experiments were carried out in an identical way to that previously reported by Reed *et al.*<sup>66</sup> using a bespoke packed-bed adsorption column constructed from Swagelok™ (Fig. 2) piping and fitting using a Jasco BP-1580-81 back pressure regulator, an Omega PX409USB High Accuracy Pressure Transducer, a 42AAV48 Midwest Pressure Systems Gas Pressure Booster, and an AND GF-1000 High Capacity 3 decimal place balance. The reactor was isolated from the system using valves and the assembly weighed on the balance. Desorption was measured by slowly opening the valves while still on the balance. Supported sorbent packed densities were measured using a Micromeritics AccuPyc 1340 Pycnometer.

Given that uptake was determined gravimetrically it was important to calculate the weight of gas present which was not interacting with the sorbent. This is known as the void space. The void space was calculated before each run took place. The accurate internal volume of the adsorber (empty) was found by water displacement (V<sub>A</sub>). The adsorber rig was then weighed (empty) and under vacuum. Quartz wool was used to ensure that packed polymers were not ejected from the adsorber, and this was also weighed. A portion of quartz wool was packed into one end of the adsorber and the polymer to be tested was then packed on top. The second portion of quartz wool was then added at the other end to seal the polymer in place and the adsorber was closed and sealed. The adsorber was then reweighed under vacuum to give the packed sorbent weight. The

volumes of the sorbent ( $V_S$ ) and quartz wool ( $V_Q$ ) were found using the density data obtained from the pycnometer measurements. These volumes were subtracted from the total internal volume to give the void space as shown in Eq. 1.

$$\text{Void Space} = V_A - (V_S + V_Q) \quad \text{Eq. 1}$$

The  $\text{CO}_2$  capacity of the sorbent was calculated using a static gas pressure and was carried out using pure  $\text{CO}_2$  gas. The starting weight of the packed adsorber was taken before the gas was introduced. Pure  $\text{CO}_2$  then enters the adsorber and the total weight increase of the system was determined ( $M_T$ ). This was achieved by closing the valves to the reactor, removing it from the system and placing it on the balance, the mass of the empty assembly having previously been measured. The mass increase was attributed to the  $\text{CO}_2$  that had been adsorbed onto the sorbent ( $M_{\text{ads}}$ ) and  $\text{CO}_2$  in the void space ( $M_{\text{void}}$ ). In order to find the mass of  $\text{CO}_2$  in the void space, the density of the gas at that specific pressure and temperature was determined. This void space mass ( $M_{\text{void}}$ ) was removed from the total mass increase ( $M_T$ ). The remaining mass ( $M_{\text{ads}}$ ) was then attributed to the gas that had adsorbed onto the sorbent (Eq. 2)

$$M_{\text{ads}} = M_T - M_{\text{void}} \quad \text{Eq.2}$$

Live IR tracking was carried out via non-dispersive infrared absorption using a CM-40401 SprintIR6S high speed  $\text{CO}_2$  sensor, capable of taking 20 readings per second accurate to 70 ppm, purchased from  $\text{CO}_2\text{Meter}$ . The detector was calibrated using a pure stream of  $\text{N}_2$  gas. Data was analysed using GasLab<sup>®</sup> version 2.0.8.14 which allowed for  $\text{CO}_2$  output to be presented as a % concentration.

## Results and Discussion

Seven hypercrosslinked polymers were synthesised from functionalised monomers all possessing different chemical moieties purposefully to see how these groups affected the  $\text{CO}_2$  uptake and selectivity at high pressure. Monomers including alcohol functionalities (triphenylmethanol and BINOL), amine functionality (2° amine carbazole and 3° amine triphenylamine), halogens (fluorobenzene) and a newly synthesised network based on dibenzyl ether which contains ether linkages were all hypercrosslinked (Figure 3). Further to this, a non-functionalised network was synthesised from polystyrene which provides a good comparison between the functionalised and non-functionalised networks. Whilst hypercrosslinked polymers made from poly(styrene),<sup>67</sup> carbazole,<sup>68</sup> BINOL,<sup>20</sup> triphenylamine<sup>69</sup> and fluorobenzene<sup>60</sup> have previously been reported, this is to our knowledge the first reported synthesis of networks synthesised from dibenzyl ether and triphenylmethanol.

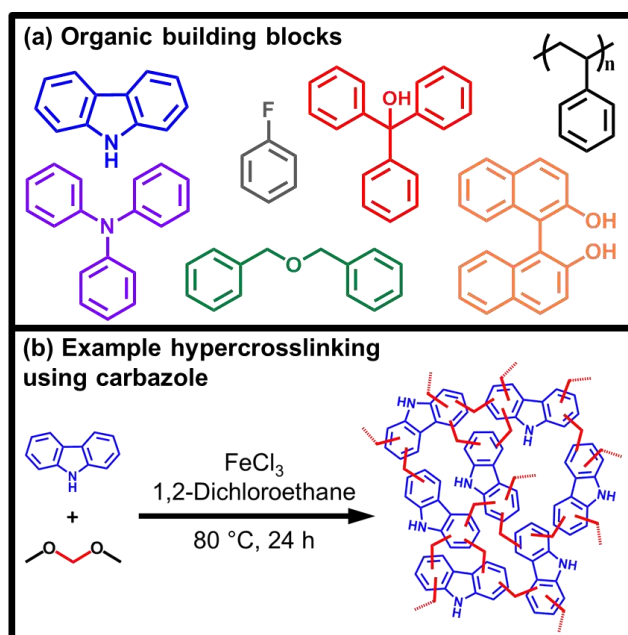


**Figure 3.** Schematic representation of HCP synthesis using the so-called external crosslinking or “knitting” method. (a) Example monomers used in this work, Poly(styrene), triphenylmethanol, BINOL, carbazole, triphenylamine, dibenzyl ether and fluorobenzene and (b) an example of the hypercrosslinking synthesis.

All networks were obtained in good yields (Table S1) similar to that found for other HCPs.<sup>20,59</sup> Structural characterisation of the HCPs was performed by elemental analysis (Table S2), infrared spectroscopy (FT-IR) (Figure S1) and <sup>13</sup>C solid state CP/MAS NMR spectroscopy (ssNMR) (Figures 4 & S2). Calculated %C, H and N of the networks were found to be typical for HCPs synthesised *via* Friedel-Crafts alkylation. There is some variation from the expected values as these are calculated assuming an idealised structure in which all protons have been exchanged for a methylene bridge. The presence of end groups and adsorbed molecules such as  $\text{CO}_2$  and water vapour may also contribute to the deviation from theoretical values. Nitrogen values of 5.17 % and 4.35 % were observed for the carbazole and triphenylamine networks respectively, indicating successful incorporation of amines into the structure.

Analysis by FTIR (Figure S1) suggests that the incorporation of the monomers into the networks with characteristic signals at *ca.* 2800  $\text{cm}^{-1}$  and 1600  $\text{cm}^{-1}$  corresponding to the, C-H and C=C stretches respectively while an additional signal at *ca.* 3500  $\text{cm}^{-1}$  is assigned to the –OH stretch in the triphenylmethanol network. An ether stretch at *ca.* 1000  $\text{cm}^{-1}$  is observed for the dibenzyl ether network.

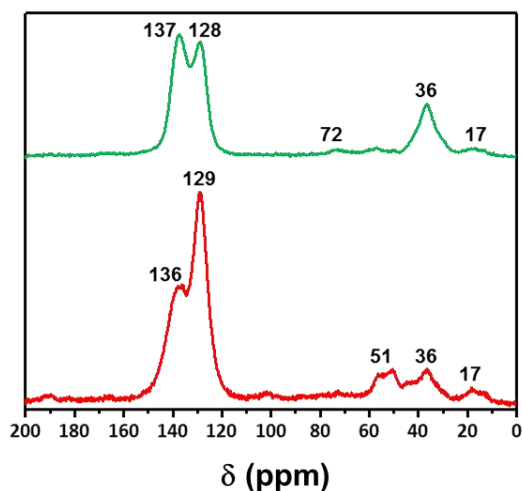


**Figure 4.** CP/MAS solid state  $^{13}\text{C}$  NMR spectra of the **dibenzyl ether** (above) and **triphenylmethanol** (below) networks

$^{13}\text{C}$  ssNMR spectra were collected for all samples and can be seen in Figure S2 whilst the spectra for the two newly synthesised materials are presented in figure 4. All networks showed two prominent signals at ca. 140 and 130 ppm corresponding to quaternary aromatic carbons ( $\text{C}_{\text{Ar}}$ ) and aromatic  $\text{C}_{\text{Ar}}\text{-H}$ . Signals at 36 ppm are assigned to methylene bridges in the networks. The resonance at 51 ppm for the triphenylmethanol network is assigned to the C-OH. For the dibenzyl ether network a resonance at 72 ppm is assigned to the  $\text{CH}_2\text{-O-CH}_2$  carbons adjacent to the ether linkage. A further resonance is observed at ca. 17 ppm and is attributed to unreacted end groups arising from the FDA crosslinker.

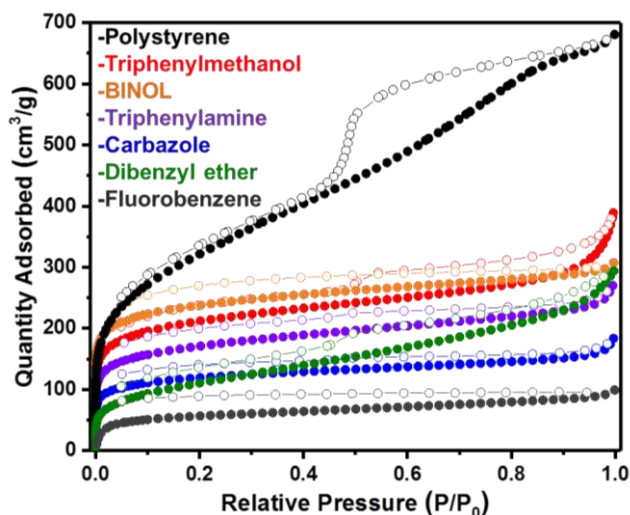


**Figure 5.** Full gas sorption isotherms for all polymer networks synthesised. Poly(styrene), **triphenylmethanol**, **BINOL**, **carbazole**, **triphenylamine** **dibenzyl ether** and fluorobenzene

The porosity of the networks was measured using nitrogen adsorption/desorption isotherms at 77 K (Figure 3). BET surface areas were calculated over a relative pressure range ( $P/P_0$ ) of 0.01–0.15 with the total pore and micropore volumes calculated at 0.95 and 0.1  $P/P_0$  respectively (Table 1). All networks adsorbed large volumes of nitrogen at low relative pressure ( $<0.1 P/P_0$ ), indicating the presence of micropores. All

networks demonstrated further uptake at higher partial pressures. This was particularly noticeable for the poly(styrene) network which demonstrates a Type II hysteresis loop on the desorb indicative of further larger (meso)pores as previously reported.<sup>67</sup>

All samples were found to be porous with surface areas ranging from 213  $\text{m}^2/\text{g}$  to 1124  $\text{m}^2/\text{g}$ . The highest surface area was found to be derived from the polystyrene network and is similar to that reported previously in the literature.<sup>67</sup> Overall the inclusion of functionality into the networks results in a lower surface area than non-functionalised HCPs. Functional 3D monomers however such as BINOL are still able to produce relatively high surface area networks. Despite their lower surface areas, the effects of the functionality are still interesting for  $\text{CO}_2$  capture and the potential for increased selectivity over nitrogen.

The total pore volumes of the materials ranged from 0.14  $\text{cm}^3/\text{g}$  to 1.01  $\text{cm}^3/\text{g}$  with the fluorobenzene and polystyrene derived HCPs showing the lowest and highest pore volumes respectively as might be expected from the highest and lowest surface area networks. As a proportion of pore volume ( $V_{0.1}/V_{\text{tot}}$ ) both carbazole and fluorobenzene showed the largest contribution of micropores while dibenzyl ether was found to have a larger proportion of meso- and macropores. It has been previously reported that smaller pores are preferential over larger pores for  $\text{CO}_2$  capture particularly at lower pressures where the uptake has not reached a maximum. It was hypothesised that the networks with a larger % of micropores may therefore be better suited towards  $\text{CO}_2$  capture than those possessing larger pores at 25 bar.<sup>70</sup>

#### Kinetic uptake of $\text{CO}_2$

High pressure  $\text{CO}_2$  adsorption experiments were conducted using the setup as previously reported by Reed and co-workers.<sup>16,66</sup> Briefly, an adsorbent was packed into a sealed unit which was exposed to high pressures of gas before being weighed to gravimetrically determine  $\text{CO}_2$  uptake. All samples were measured three times and an average of the data was taken and used. All measurements on the functionalised HCPs were recorded at 40  $^\circ\text{C}$  to more closely match cooled flue gas temperatures from industrial sources. The stack temperature can vary depending on the process but can be 120  $^\circ\text{C}$  for post-combustion processes, 250-350  $^\circ\text{C}$  from steel plants and over 1000  $^\circ\text{C}$  for smelting works. As such, the flue gas temperatures need to be reduced to values where absorption or adsorption are feasible. Moisture vapour is also an important consideration when for post-combustion capture,<sup>4,19</sup> therefore all samples were tested under “wet” conditions. More specifically, after synthesis the samples were dried under vacuum at 60  $^\circ\text{C}$  before being allowed to adsorb moisture from the air at 40-50% humidity for at least 24 h before all adsorption measurements. These conditions allow for results more comparable to those used in industry where gas mixtures are hydrated.

Pressures of 10 and 20 bar are typical pressures for PSA which are easily attainable without a significant increase in plant operating costs. The rate at which each network reached

**Table 1.** Gas sorption properties for all polymer networks

Functional group	Polymer	SA <sub>BET</sub> (m <sup>2</sup> /g) <sup>a</sup>	V <sub>tot</sub> (cm <sup>3</sup> /g) <sup>b</sup>	V <sub>0.1</sub> (cm <sup>3</sup> /g) <sup>c</sup>	V <sub>0.1</sub> /V <sub>tot</sub>
N/A	Poly(styrene)	1124	1.01	0.42	0.42
-OH	Triphenylmethanol	781	0.48	0.30	0.63
	BINOL	888	0.45	0.35	0.70
R-O-R	Dibenzyl ether	397	0.39	0.14	0.36
-NR <sub>x</sub>	Carbazole	445	0.24	0.17	0.71
	Triphenylamine	630	0.37	0.24	0.65
-X	Fluorobenzene	213	0.14	0.10	0.71

<sup>a</sup> Apparent BET surface areas were determined over the pressure range (P/P<sub>0</sub>) = 0.01 – 0.15. <sup>b</sup> Total pore volume calculated at 0.99 P/P<sub>0</sub> <sup>c</sup> Micropore volume calculated at 0.1 P/P<sub>0</sub>

saturation at 10 and 20 bar was therefore measured (Figure 6). At 20 bar all HCP networks become fully saturated rapidly with t<sub>90</sub> values (the time at which 90% of the total uptake is completed), of 85 seconds or less (Table S5), while at the lower pressure of 10 bar the time to reach saturation was up to 3 mins with the hydrophilic networks triphenylalcohol and BINOL taking longest and the hydrophobic networks poly(styrene) and fluorobenzene the shortest. The rapid sorption period is advantageous should these materials be applied to an industrial PSA approach given that the less time the material has to spend at elevated pressures to greater the economic and energy benefit.

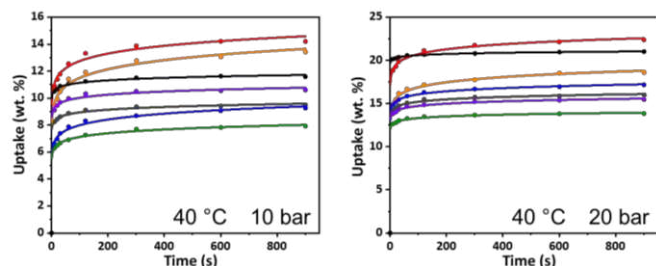


**Figure 6.** Kinetic studies of CO<sub>2</sub> uptake, for each functionalised polymer network at 40 °C and 10 bar (left) and 20 bar (right). HCPs colours are as follows: Poly(styrene), triphenylmethanol, BINOL, carbazole, triphenylamine, dibenzyl ether and fluorobenzene

At 10 bar the two -OH containing networks (Triphenylmethanol and BINOL) perform the best reporting final uptakes of around 13 and 14 % wt. respectively. Alcohol containing porous polymers have previously been shown to demonstrate good CO<sub>2</sub> capture capabilities, these measurements further demonstrate the advantage of such functionalities at higher pressures.<sup>20,71</sup> The highest surface area material – the non-functional poly(styrene) shows uptake at 10 bar at around 11 % wt. This material has a much higher surface area than the two alcohol materials yet still underperforms in comparison to the alcohol networks. At the same time this non-functionalised network outperforms other functionalities, demonstrating that both surface area and functionality is important when designing materials for CCS. The amine containing networks, (triphenylamine and carbazole) and the two other networks, (fluorobenzene and the newly synthesised dibenzyl ether), all perform less well with uptakes ranging from 6 % wt. to 10 % wt.

At 20 bar all samples show increased uptake of CO<sub>2</sub> compared to 10 bar. The triphenylmethanol network continues to show the highest final uptake of around 22 % wt., yet at this elevated pressure the poly(styrene) network is the second best performing material with an uptake of just over 20 % wt. The BINOL network shows a final uptake of just under 17 % wt. The reversal of these two materials may demonstrate that at higher pressures, higher surface area may

be more advantageous than chemical functionality. Though, should this be true then, one may expect the fluorobenzene network to show the lowest uptake given its low surface area. In fact, the fluorobenzene network and the triphenylamine network show similar uptakes despite having a surface area being almost 3× lower for fluorobenzene. In this case we attribute the effect to the presence of water which is co-adsorbed in each network. It is known that the presence of water can be detrimental to CO<sub>2</sub> adsorption and the presence of the hydrophobic fluoride functionality may aid the adsorption of CO<sub>2</sub> by the network compared to the higher surface area hydrophilic amine functionalised triphenylamine network. The newly synthesised dibenzyl ether network shows the poorest uptake at ~12 % wt. This poor performance, despite a reasonable surface area, could be somewhat due to the presence of larger pore sizes dominating the material. In comparison, the triphenylmethanol, carbazole and fluorobenzene networks have a greater proportion of smaller micropores aiding their uptake under these conditions.

### Selectivity measurements

In order to investigate how selective the networks were for CO<sub>2</sub> over that of the major component of flue gas (N<sub>2</sub>), the uptake of both CO<sub>2</sub> and N<sub>2</sub> was measured for each HCP network at pressures between 5 and 25 bar at a temperature of 40 °C (Figures S4 & S5). HCP networks were exposed to a pressurised stream of either pure CO<sub>2</sub> or N<sub>2</sub> for a 5-minute adsorption period, the time at which the previous kinetic runs showed to be sufficient for equilibration, after which the gravimetric uptake was recorded and the average uptake calculated over three runs. Using these experiments it is possible to estimate the CO<sub>2</sub>:N<sub>2</sub> selectivity of the networks at high pressures typical for PSA.

**Table 2.** Average CO<sub>2</sub> and N<sub>2</sub> uptake capabilities for all polymer networks at 40 °C at both 5 and 25 bar

Material	CO <sub>2</sub> Uptake @ 40 °C (wt. %)		N <sub>2</sub> Uptake @ 40 °C (wt. %)	
	5 bar	25 bar	5 bar	25 bar
Poly(styrene)	5.90	25.08	2.44	9.88
Triphenylmethanol	6.37	28.94	1.65	7.36
BINOL	7.04	24.03	2.00	7.67
Dibenzyl ether	4.46	17.95	1.01	3.96
Carbazole	5.08	19.76	1.36	3.11
Triphenylamine	5.18	20.96	1.44	4.84
Fluorobenzene	4.47	18.21	2.10	5.76

All of the networks demonstrated much higher uptakes of CO<sub>2</sub> than N<sub>2</sub> under identical adsorption conditions (Table 2), typically > 3–5× higher than the respective N<sub>2</sub> uptake thereby demonstrating a preference to adsorb CO<sub>2</sub> over N<sub>2</sub>. The CO<sub>2</sub> uptake at 25 bar is in line with the kinetic uptakes at 20 bar which shows the triphenylmethanol and poly(styrene) networks to be the best performing materials with uptake exceeding 25 % wt., while the dibenzyl ether network showed the lowest uptake of below 18 % wt. The nitrogen uptake of the networks correlates well with the BET surface areas of the materials, exhibiting no strong interaction with the network surface functionalities except for the hydrophobic fluorobenzene network which shows higher N<sub>2</sub> uptake than three networks with higher surface areas which we attribute to the relative hydrophobicity of the fluorobenzene network.

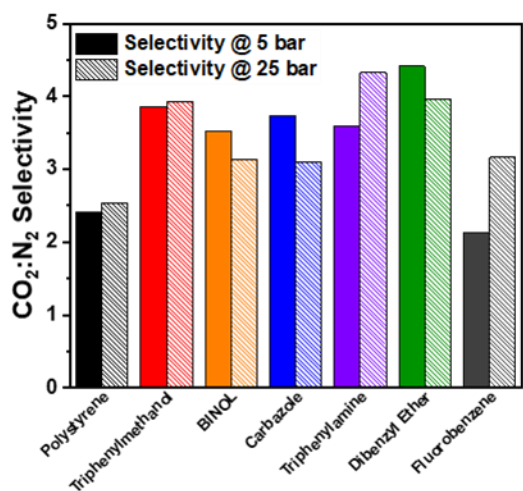
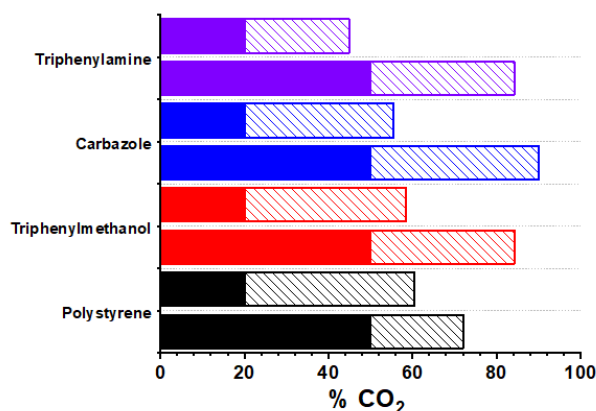


**Figure 7.** CO<sub>2</sub>:N<sub>2</sub> selectivity of networks at 40 °C and 5 bar (solid bars) and 25 bar (dashed bars).

The selectivities for each network were calculated from the CO<sub>2</sub> and N<sub>2</sub> uptakes at 5 and 25 bar (Figure 7) with those for the functional networks shown to be generally higher than for the non-functionalised, yet high surface area, poly(styrene) network. Interestingly the operating pressure has little effect on the overall selectivity of the networks with the selectivity at 5 bar similar to that at 25 bar. At 5 bar the dibenzyl ether network showed the highest selectivity, while at the higher pressure of 25 bar used for PSA the triphenylamine network was found to have the highest selectivity of 4:1. Both the alcohol containing triphenylamine and BINOL networks showed good selectivities of around 4:1 and 3.5:1 respectively which combined with their high CO<sub>2</sub> uptake would make them the most promising materials for PSA.

Whilst some insight into the selectivity of the materials can be derived using pure gas streams, the use of mixed gas streams is more representative of actual industrial flue gas. To investigate how the materials performed at enriching a CO<sub>2</sub> stream the most promising materials were exposed to a gas mix



comprised of an 80:20 N<sub>2</sub>:CO<sub>2</sub> at 40 °C and 20 bar for 5 minutes. The concentration of CO<sub>2</sub> in the output gas was measured at 20 bar, after which the pressure was then released from the adsorber. When the pressure reaches 1 bar the concentration of CO<sub>2</sub> was calculated by IR. Finally, the same experiment was repeated using a stream comprised of 50:50 N<sub>2</sub>:CO<sub>2</sub> mix at 40 °C (Figure 8). This test would replicate two cycles whereby the output from the first cycle is fed back in to the PSA setup and the method is repeated once again.

**Figure 8.** CO<sub>2</sub> concentration of the input gas (solid bar) and the output exhaust gas stream at 1 bar (dashed bars) at 40 °C.

Initially, when the chosen samples were exposed to an 80:20 N<sub>2</sub>:CO<sub>2</sub> stream all materials were able to selectively adsorb the CO<sub>2</sub> at 20 bar and then desorb it at 1 bar. This resulted in the successful separation of CO<sub>2</sub> from N<sub>2</sub> and the generation of a gas stream enriched to over 50% CO<sub>2</sub> in the case of triphenylmethanol, poly(styrene) and carbazole after one cycle. We therefore exposed the materials to a 50:50 N<sub>2</sub>:CO<sub>2</sub> stream, the equivalent of feeding the stream from the first test back into the materials and repeated the experiment again. The triphenylmethanol and triphenylamine samples were able to enrich the stream of gas to over 80% CO<sub>2</sub>. This experiment demonstrates that these materials are able to take a dilute stream of flue gas and, after two pressure swing cycles, convert this dilute stream into a concentrated CO<sub>2</sub> stream by preferential adsorption of CO<sub>2</sub> over N<sub>2</sub>.

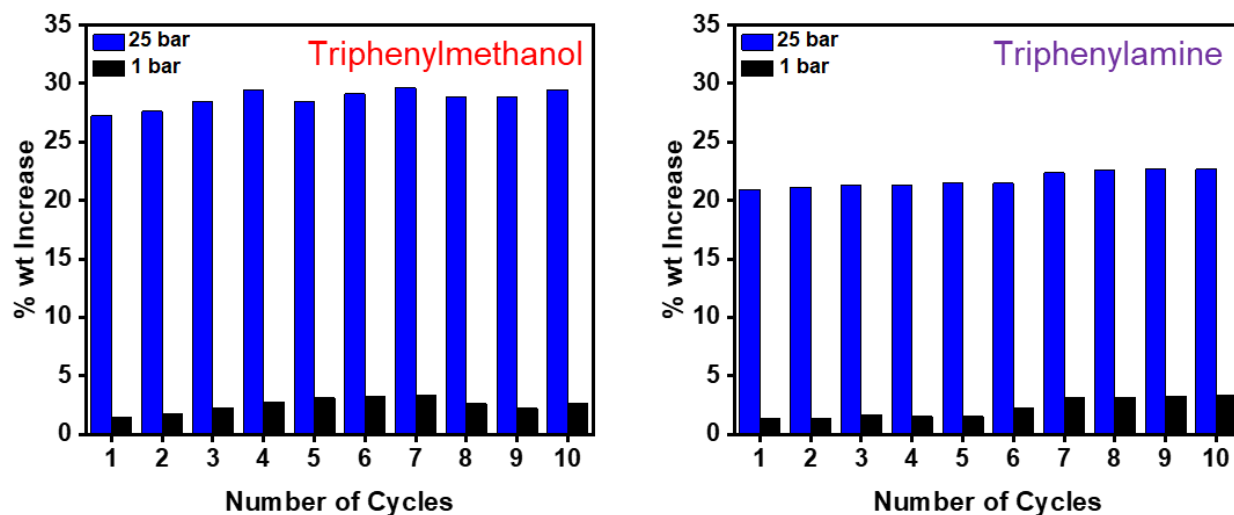


Figure 9. Recyclability studies for triphenylmethanol (left) and triphenylamine (right) networks during 10 adsorb/desorb cycles of CO<sub>2</sub> at 25 bar and 40 °C.

Finally, the ability of the sorbents to be used over repeat adsorption-desorption cycles was tested using the best performing triphenylmethanol and triphenylamine networks (Figure 9). These networks were exposed to a 25 bar stream of CO<sub>2</sub> before having the pressure reduced to 1 bar with the uptakes at each pressure recorded and was repeated for 10 cycles. Importantly, as in a typical PSA process the materials were not exposed to a vacuum between runs to remove any CO<sub>2</sub> as not to further increase the energy demands of the process. Both materials reached a maximum uptake at 25 bar and this was found to be reproducible over the 10 cycle run demonstrating no loss in performance over time. Both samples retained some gas at 1 bar though this quantity was minimal (<3% wt.) and had no significant effect on the uptake at higher pressures.

## Conclusion

To conclude, a series of functional porous materials synthesised via conventional hypercrosslinking chemistry were applied as sorbents to selectively separate out CO<sub>2</sub> from simulated flue gas mixes. The uptake capacity, uptake rate and CO<sub>2</sub>:N<sub>2</sub> selectivity at high pressure were all thoroughly examined in order to test the materials at high pressure and using a pressure swing approach. The best performing materials were then taken forward and applied towards actual pressure swing separation experiments using simulated gas mixtures representative of those in industry. Finally, the recyclability of the optimum materials were tested to investigate if their performance was hindered after multiple adsorb/desorb cycles. All materials were found to uptake CO<sub>2</sub> rapidly with most of the uptake being complete within 2 minutes with the -OH functionalised and non-functional poly(styrene) network showing the highest CO<sub>2</sub> capacity. Due to their high and selective uptakes both the triphenylmethanol and triphenylamine networks were taken forward and applied to an actual pressure swing approach where it was found that after only two cycles they were able to convert a 20% CO<sub>2</sub> stream into one exceeding 85% CO<sub>2</sub>. This was an excellent example of how cheaply synthesised porous materials can be easily synthesised and applied to a pressure swing methodology demonstrating excellent CO<sub>2</sub>:N<sub>2</sub>

capabilities. It is hoped that this work inspires more research into PSA techniques so as to improve on the current energy intensive and fiscally demanding temperature swing techniques rife throughout industry.

## Conflicts of interest

There are no conflicts to declare.

## Acknowledgements

PS would like to thank the ESPRC for funding of the CO<sub>2</sub>Chem Grand Challenge Network (EP/K007947/1 and EP/P026435/1). Dr. Sandra van Meurs is thanked for running solid state NMR samples.

## Notes and references

- 1 International Energy Agency, *World Energy Outlook 2008*, 2008, vol. 23.
- 2 M. E. Boot-Handford, J. C. Abanades, E. J. Anthony, M. J. Blunt, S. Brandani, N. Mac Dowell, J. R. Fernandez, M.-C. Ferrari, R. Gross, J. P. Hallett, R. S. Haszeldine, P. Heptonstall, A. Lyngfelt, Z. Makuch, E. Mangano, R. T. J. Porter, M. Pourkashanian, G. T. Rochelle, N. Shah, J. G. Yao and P. S. Fennell, *Energy Environ. Sci.*, 2014, **7**, 130–189.
- 3 A. Samanta, A. Zhao, G. K. H. Shimizu, P. Sarkar and R. Gupta, *Ind. Eng. Chem. Res.*, 2012, **51**, 1438–1463.
- 4 T. C. Drage, C. E. Snape, L. A. Stevens, J. Wood, J. Wang, A. I. Cooper, R. Dawson, X. Guo, C. Satterley and R. Irons, *J. Mater. Chem.*, 2012, **22**, 2815–2823.
- 5 A. J. Reynolds, T. V. Verheyen, S. B. Adeloju, E. Meuleman and P. Feron, *Environ. Sci. Technol.*, 2012, **46**, 3643–3654.
- 6 M. Oschatz and M. Antonietti, *Energy Environ. Sci.*, 2017, **11**, 57–70.
- 7 D. M. D'Alessandro, B. Smit and J. R. Long, *Angew. Chemie Int. Ed.*, 2010, **49**, 6058–6082.
- 8 J. Wang, L. Huang, R. Yang, Z. Zhang, J. Wu, Y. Gao, Q.

- Wang, D. O'Hare and Z. Zhong, *Energy Environ. Sci.*, 2014, **7**, 3478–3518.
- 9 P. Luis, *Desalination*, 2016, **380**, 93–99.
- 10 O. Aschenbrenner and P. Styring, *Energy Environ. Sci.*, 2010, **3**, 1106–1113.
- 11 J. Schell, N. Casas, D. Marx and M. Mazzotti, *Ind. Eng. Chem. Res.*, 2013, **52**, 8311–8322.
- 12 L. Riboldi and O. Bolland, *Energy Procedia*, 2017, **114**, 2390–2400.
- 13 P. Markewitz, W. Kuckshinrichs, W. Leitner, J. Linssen, P. Zapp, R. Bongartz, A. Schreiber and T. E. Müller, *Energy Environ. Sci.*, 2012, **5**, 7281.
- 14 M. Abu Ghali and Y. Dahman, *Energy Technol.*, 2017, **5**, 356–372.
- 15 M. Ding, R. W. Flaig, H.-L. Jiang and O. M. Yaghi, *Chem. Soc. Rev.*, 2019, **48**, 2783–2828.
- 16 G. R. M. Dowson, D. G. Reed, J.-M. Bellas, C. Charalambous and P. Styring, *Faraday Discuss.*, 2016, **192**, 511–527.
- 17 S. Supasitmongkol and P. Styring, *Energy Environ. Sci.*, 2010, **3**, 1961–1972.
- 18 L. Tan and B. Tan, *Chem. Soc. Rev.*, 2017, **46**, 3322–3356.
- 19 R. T. Woodward, L. A. Stevens, R. Dawson, M. Vijayaraghavan, T. Hasell, I. P. Silverwood, A. V Ewing, T. Ratvijitvech, J. D. Exley, S. Y. Chong, F. Blanc, D. J. Adams, S. G. Kazarian, C. E. Snape, T. C. Drage and A. I. Cooper, *J. Am. Chem. Soc.*, 2014, **136**, 9028–9035.
- 20 R. Dawson, L. A. Stevens, T. C. Drage, C. E. Snape, M. W. Smith, D. J. Adams and A. I. Cooper, *J. Am. Chem. Soc.*, 2012, **134**, 10741–10744.
- 21 C. F. Martin, E. Stöckel, R. Clowes, D. J. Adams, A. I. Cooper, J. J. Pis, F. Rubiera and C. Pevida, *J. Mater. Chem.*, 2011, **21**, 5475–5483.
- 22 R. Dawson, A. I. Cooper and D. J. Adams, *Polym. Int.*, 2013, **62**, 345–352.
- 23 R. Dawson, E. Stöckel, J. R. Holst, D. J. Adams and A. I. Cooper, *Energy Environ. Sci.*, 2011, **4**, 4239–4245.
- 24 R. Dawson, D. J. Adams and A. I. Cooper, *Chem. Sci.*, 2011, **2**, 1173–1177.
- 25 J. X. Jiang, F. Su, A. Trewin, C. D. Wood, N. L. Campbell, H. Niu, C. Dickinson, A. Y. Ganin, M. J. Rosseinsky, Y. Z. Khimyak and A. I. Cooper, *Angew. Chemie - Int. Ed.*, 2007, **46**, 8574–8578.
- 26 J. Schmidt, M. Werner and A. Thomas, *Macromolecules*, 2009, **42**, 4426–4429.
- 27 D. J. Woods, R. S. Sprick, C. L. Smith, A. J. Cowan and A. I. Cooper, *Adv. Energy Mater.*, 2017, **1700479**, 1700479.
- 28 J. L. Segura, M. J. Mancheño and F. Zamora, *Chem. Soc. Rev.*, 2016, **45**, 5635–5671.
- 29 A. P. Cote, A. I. Benin, N. W. Ockwig, M. O'Keeffe, A. J. Matzger and O. M. Yaghi, *Science (80-. )*, 2005, **310**, 1166–1170.
- 30 S. Dalapati, S. Jin, J. Gao, Y. Xu, A. Nagai and D. Jiang, *J. Am. Chem. Soc.*, DOI:10.1021/ja4103293.
- 31 P. Kuhn, M. Antonietti and A. Thomas, *Angew. Chemie Int. Ed.*, 2008, **47**, 3450–3453.
- 32 A. Bhunia, D. Esquivel, S. Dey, R. Fernández-Terán, Y. Goto, S. Inagaki, P. Van Der Voort and C. Janiak, *J. Mater. Chem. A*, 2016, **4**, 13450–13457.
- 33 Y. Fu, W. Yu, W. Zhang, Q. Huang, J. Yan, C. Pan and G. Yu, *Polym. Chem.*, 2018, **9**, 4125–4131.
- 34 P. M. Budd, B. S. Ghanem, S. Makhseed, N. B. McKeown, K. J. Msayib and C. E. Tattershall, *Chem. Commun.*, 2004, 230.
- 35 N. B. McKeown, *ISRN Mater. Sci.*, 2012, **2012**, 1–16.
- 36 P. M. Budd, K. J. Msayib, C. E. Tattershall, B. S. Ghanem, K. J. Reynolds, N. B. McKeown and D. Fritsch, *J. Memb. Sci.*, 2005, **251**, 263–269.
- 37 D. Ramimoghdam, E. M. Gray and C. J. Webb, *Int. J. Hydrogen Energy*, 2016, **41**, 16944–16965.
- 38 H. Ma, B. Li, L. Zhang, D. Han and G. Zhu, *J. Mater. Chem. A*, 2015, **3**, 19346–19352.
- 39 A. Deshmukh, S. Bandyopadhyay, A. James and A. Patra, *J. Mater. Chem. C*, 2016, **4**, 4427–4433.
- 40 X. Wu, H. Li, B. Xu, H. Tong and L. Wang, *Polym. Chem.*, 2014, **5**, 4521–4525.
- 41 J. Luo, J. Lu and J. Zhang, *J. Mater. Chem. A*, 2018, **6**, 15154–15161.
- 42 R. M. N. Kalla, M.-R. Kim and I. Kim, *Ind. Eng. Chem. Res.*, 2018, **57**, 11583–11591.
- 43 R. Li, Z. J. Wang, L. Wang, B. C. Ma, S. Ghasimi, H. Lu, K. Landfester and K. A. I. Zhang, *ACS Catal.*, 2016, **6**, 1113–1121.
- 44 J. X. Jiang, C. Wang, A. Laybourn, T. Hasell, R. Clowes, Y. Z. Khimyak, J. Xiao, S. J. Higgins, D. J. Adams and A. I. Cooper, *Angew. Chemie - Int. Ed.*, 2011, **50**, 1072–1075.
- 45 B. Li, F. Su, H.-K. Luo, L. Liang and B. Tan, *Microporous Mesoporous Mater.*, 2011, **138**, 207–214.
- 46 Z. Li, H. Li, H. Xia, X. Ding, X. Luo, X. Liu and Y. Mu, *Chem. - A Eur. J.*, 2015, **21**, 17355–17362.
- 47 R. X. Yang, T. T. Wang and W. Q. Deng, *Sci. Rep.*, 2015, **5**, 1–9.
- 48 A. M. James, S. Harding, T. Robshaw, N. Bramall, M. D. Ogden and R. Dawson, *ACS Appl. Mater. Interfaces*, 2019, **11**, 22464–22473.
- 49 W. Lu, J. P. Sculley, D. Yuan, R. Krishna, Z. Wei and H.-C. Zhou, *Angew. Chemie Int. Ed.*, 2012, **51**, 7480–7484.
- 50 R. M. Gulam, T. E. Reich, R. Kassab, K. T. Jackson and H. M. El-Kaderi, *Chem. Commun.*, 2012, **48**, 1141–1143.
- 51 T. Ben, H. Ren, S. Ma, D. Cao, J. Lan, X. Jing, W. Wang, J. Xu, F. Deng, J. M. Simmons, S. Qiu and G. Zhu, *Angew. Chemie*, 2009, **121**, 9621–9624.
- 52 D. Yuan, W. Lu, D. Zhao and H.-C. Zhou, *Adv. Mater.*, 2011, **23**, 3723–3725.
- 53 Y. Liu, S. Wu, G. Wang, G. Yu, J. Guan, C. Pan and Z. Wang, *J. Mater. Chem. A*, 2014, **2**, 7795–7801.
- 54 R. Dawson, A. I. Cooper and D. J. Adams, *Prog. Polym. Sci.*, 2012, **37**, 530–563.
- 55 S. Xu, Y. Luo and B. Tan, *Macromol. Rapid Commun.*, 2013, **34**, 471–84.
- 56 J. Huang and S. R. Turner, *Polym. Rev.*, 2018, **58**, 1–41.
- 57 N. Fontanals, J. Cortés, M. Galià, R. Maria Marcé, P. A. G. Cormack, F. Borrull and D. C. Sherrington, *J. Polym. Sci. Part A Polym. Chem.*, 2005, **43**, 1718–1728.
- 58 J.-Y. Lee, C. D. Wood, D. Bradshaw, M. J. Rosseinsky and A. I. Cooper, *Chem. Commun.*, 2006, 2670.

- 59 B. Li, R. Gong, W. Wang, X. Huang, W. Zhang, H. Li, C. Hu and B. Tan, *Macromolecules*, 2011, **44**, 2410–2414.
- 60 C. Wilson, M. J. Main, N. J. Cooper, M. E. Briggs, A. I. Cooper and D. J. Adams, *Polym. Chem.*, 2017, **8**, 1914–1922.
- 61 X. Yang, M. Yu, Y. Zhao, C. Zhang, X. Wang and J. X. Jiang, *RSC Adv.*, 2014, **4**, 61051–61055.
- 62 L. Tan, B. Li, X. Yang, W. Wang and B. Tan, *Polymer (Guildf.)*, 2015, **70**, 336–342.
- 63 R. Dawson, T. Ratvijitvech, M. Corker, A. Laybourn, Y. Z. Khimyak, A. I. Cooper and D. J. Adams, *Polym. Chem.*, 2012, **3**, 2034–2038.
- 64 W. Wang, M. Zhou and D. Yuan, *J. Mater. Chem. A*, 2017, **5**, 1334–1347.
- 65 D. S. Ahmed, G. A. El-Hiti, E. Yousif, A. A. Ali and A. S. Hameed, *J. Polym. Res.*, , DOI:10.1007/s10965-018-1474-x.
- 66 D. G. Reed, G. R. M. Dowson and P. Styring, *Front. Energy Res.*, 2017, **5**, 1–12.
- 67 T. Ratvijitvech, M. Barrow, A. I. Cooper and D. J. Adams, *Polym. Chem.*, 2015, **6**, 7280–7285.
- 68 X. Zhu, S. M. Mahurin, S.-H. An, C.-L. Do-Thanh, C. Tian, Y. Li, L. W. Gill, E. W. Hagaman, Z. Bian, J.-H. Zhou, J. Hu, H. Liu and S. Dai, *Chem. Commun.*, 2014, **50**, 7933.
- 69 D. Zhang, L. Tao, Q. Wang and T. Wang, *Polymer (Guildf.)*, 2016, **82**, 114–120.
- 70 F. R. and C. P. Claudia F. Martín, Ev Stöckel, Rob Clowes, Dave J. Adams, Andrew I. Cooper, Jose J. Pis, *J. Mater. Chem.*, 2011, **21**, 5475–5483.
- 71 S. Yao, X. Yang, M. Yu, Y. Zhang and J.-X. Jiang, *J. Mater. Chem. A*, 2014, **2**, 8054–8059.